Title
Mesenchymal Stem Cell–Derived Extracellular Vesicles Decrease Lung Injury in Mice

Journal
The Journal of Immunology, 203(7)

ISSN
0022-1767

Authors
Hao, Qi
Gudapati, Varun
Monsel, Antoine
et al.

Publication Date
2019-10-01

DOI
10.4049/jimmunol.1801534

Peer reviewed

Published in final edited form as:

J Immunol. 2019 October 01; 203(7): 1961–1972. doi:10.4049/jimmunol.1801534.

Mesenchymal Stem Cell-Derived Extracellular Vesicles Decrease Lung Injury in Mice

Qi Hao[1], **Varun Gudapati**[1], **Antoine Monsel**[1], **Jeong H. Park**[1], **Shuling Hu**[1], **Hideya Kato**[1], **Jae H. Lee**[1], **Li Zhou**[1], **Hongli He**[1], **Jae W. Lee**[1]

[1]University of California San Francisco, Department of Anesthesiology, San Francisco, CA 94143

Abstract

Human mesenchymal stem cell (MSC) extracellular vesicles (EV) can reduce the severity of bacterial pneumonia, but little is known about the mechanisms underlying their antimicrobial activity. In the current study, we found that bacterial clearance induced by MSC EV in *E.coli* pneumonia in C57BL/6 mice was associated with high levels of leukotriene (LT) B_4 in the injured alveolus. More importantly, the antimicrobial effect of MSC EV was abrogated by co-treatment with a LTB_4 BLT1 antagonist. To determine the role of MSC EV on leukotriene metabolism, we measured the effect of MSC EV on a known ATP-binding cassette transporter, multidrug resistance-associated protein 1 (MRP1), and found that MSC EV suppressed MRP1 mRNA, protein, and pump function in LPS stimulated Raw264.7 cells *in vitro*. The synthesis of LTB_4 and LTC_4 from LTA_4 are competitive, and MRP1 is the efflux pump for LTC_4. Inhibition of MRP1 will increase LTB_4 production. In addition, administration of a nonspecific MRP1 inhibitor (MK-571) reduced LTC_4 and subsequently increased LTB_4 levels in C57BL/6 mice with acute lung injury, increasing overall antimicrobial activity. We previously found that the biological effects of MSC EV were through the transfer of its content, such as mRNA, miroRNA, and proteins, to target cells. In the current study, miR-145 knockdown abolished the effect of MSC EV on the inhibition of MRP1 *in vitro* and the antimicrobial effect *in vivo*. In summary, MSC EV suppressed MRP1 activity through transfer of miR-145, thereby resulting in enhanced LTB_4 production and antimicrobial activity through LTB_4/BLT1 signaling.

Keywords

Acute lung injury; extracellular vesicles; leukotriene B_4; mesenchymal stem cells; MRP1; miR-145

Address correspondence and reprint requests to Dr. Jae-Woo Lee. Department of Anesthesiology, University of California San Francisco, 505 Parnassus Ave., Box 0648, San Francisco, California 94143, USA. jae-woo.lee@ucsf.edu.

Q.H. and J.W.L. designed experiments. Q.H., V.G., A.M., J.P., S.H., H.K., J.H.L., L.Z., and H.H. performed the experiments. Q.H. and J.W.L. wrote the manuscript. J.W.L. had final approval of the manuscript.

Disclosures

The authors have declared that no conflict of interest exists.

Introduction

Leukotrienes (LTs) are a family of lipid mediators associated with acute and chronic inflammatory diseases. They act in host defense, intercellular communication, and signal transduction. LTs include LTB_4 and cysteinyl LTs (CysLTs) (LTC_4, LTD_4, and LTE_4) (1). CysLTs play a significant role in the pathogenesis of inflammatory related diseases. In asthma, they mediate bronchoconstriction, bronchial hyperactivity, edema, and eosinophilia (2,3). LTB_4 was initially identified as an activator of granulocytes (4) and is known to exert broad pro-inflammatory effects (5,6). Multiple studies have demonstrated the antimicrobial effects of LTB_4, which may be mediated through augmented phagocytosis and the release of antimicrobial agents (7,8). LTB_4 can enhance host defense against pneumonia and sepsis (9-12). The biosynthesis of LTs occurs predominantly in leukocytes. In response to stimuli (immune and inflammatory signals), arachidonic acid (AA) is liberated from membrane phospholipids, catalyzed by phospholipase A_2 (PLA_2). AA is then converted to LTA_4 via the action of 5-lipoxygenase. From LTA_4 there are two competitive metabolic routes leading to the synthesis of LTB_4 or LTC_4 via the enzymes LTA_4 hydrolase (LTA_4H) or LTC_4 synthase (LTC_4S) respectively. LTC_4 is transported across the plasma membrane by MRP1, also named ABCC1, and subsequently converted into LTD_4 and LTE_4 in the extracellular space.

MRP1 is a member of the ATP-binding cassette transporter superfamily along with multidrug resistance protein 1 (MDR1), also named ABCB1 or P-glycoprotein. MRP1 is a ~190 kDa membrane protein and functions as a transporter. LTC_4 is a particularly high-affinity substrate of MRP1 (13,14), and MRP1 is the major efflux pump for LTC_4 (15). In leukotriene-mediated inflammation, MRP1 plays a crucial role in LTC_4 release (9,16). Surprisingly, mice lacking *Mrp1* are more resistant to bacterial pneumonia compared to wild type mice (9). Due to a lack of *Mrp1* expression, efflux of LTC_4 is impaired and intracellular LTC_4 is accumulated (9). Accumulated LTC_4 down-regulates LTC_4S thus increasing the availability of LTA_4 for LTA_4H. LTA_4 thus becomes more available for conversion to LTB_4 leading to enhanced LTB_4 release (17). In addition, LTA_4H, which can also be released into the extracellular space, possesses significant aminopeptidase activity against the matrikine, proline-glycine-proline (PGP) (18). PGP is generated from the extracellular matrix (ECM) collagen, via enzymes such as matrix metalloproteinase (MMP)-9, followed by cleavage by prolyl endopeptidase (PE) (19). The degradation of PGP by LTA_4H help facilitates the resolution of inflammation (18) (Fig. 1). The extracellular role of LTA_4H in suppressing inflammation through PGP degradation has been reported in various pulmonary disorders (18,20-22).

Human MSC EV have been studied in various acute lung injury models as a therapeutic due to their ability to reduce inflammation, decrease lung permeability, and reduce bacterial pneumonia (23-26). However, the mechanism underlying the antimicrobial activity of MSC EV remains largely unknown. MSC derived EV are small membrane bound vesicles, originating from intracellular multi-vesicles or from budding off the plasma membrane. MSC and MSC EV contain numerous proteins and RNA. The RNA components carried by MSC EV are mainly small RNAs (<100 bp) including miRs (27-29). MiRs regulate gene expression and function not only within the cells where they are transcribed but can be transferred to target cells to mediate gene expression and regulate cell function (30).

MiR-145 has been found in MSC cells (31,32), MSC conditioned medium (CM) (29) and MSC derived exosomes (27), and it is one of the top 10 most abundant miRs detected (27). Recently miR-145 was found to directly regulate MRP1 expression in breast cancer (33) and gallbladder cancer (34).

In the present study, we hypothesized that miR-145 present in MSC EV may reduce MRP1 expression in leukocytes and subsequently enhance the production of LTB_4 and increase overall antimicrobial activity.

Materials and Methods

Mesenchymal Stem Cell Extracellular Vesicle Isolation and Characterization

Human MSC were obtained from a National Institutes of Health repository from Texas A&M Health Science Center (Temple, TX). Human bone marrow derived MSC, from three different donors, with passages 3–8 were used in this study. These human MSC were well characterized (23,35). Their capability for osteogenic, adipogenic, and chondrogenic lineage differentiation were previously demonstrated. Flow cytometry results showed > 99% cells display the standard MSC surface markers such as CD105, CD90, CD73, CD44, and CD166. Their phenotype and function met all the criteria for MSC as defined by the International Society of Cellular Therapy (36). Normal adult human lung fibroblasts (NHLF) were used as cellular controls (Lonza Group, Basel, Switzerland).

EV were obtained from the supernatants of MSC and NHLF using ultracentrifugation as previously described (23,37). Briefly, MSC or NHLF were cultured until confluent and then serum starved for 48 h in fresh conditioned medium without FBS but containing 0.5% BSA (MP Biomedicals, LLC, Solon, OH). To isolate EV, the conditioned medium of MSC or NHLF was centrifuged at 3,000 rpm for 20 min to remove cellular debris and then at 100,000 g (Beckman Coulter, Brea, CA) to sediment the EV for 1 h at 4 ºC. The EV were washed in PBS and then submitted to a second ultracentrifugation before being re-suspended according to the final cell count after 48 h of serum starvation (10 μl per 1×10^6 cells).

MSC EV were characterized by morphology, size, protein, RNA content, and surface receptor. MSC EV were examined by electron microscopy for morphology and approximate size. Both size distribution (both mean and modal) and the concentration of MSC EV as reconstituted in PBS were analyzed by nanoparticle tracking (NPT) analysis with NanoSight NS300 (Malvern Instruments, Malvern, United Kingdom). This technique calculates size based on tracking of Brownian motion and concentration by particle observation on a frame-by-frame basis by the high-sensitivity sCMOS camera. Data were analyzed with NTA2.3 software. The content of total protein and RNA of MSC EV were quantified by BCA protein assay, Western blot, and RT-PCR. To characterize the surface molecules, MSC EV were fluorescently labeled with PKH26 dye (Sigma-Aldrich, St. Louis, MO, USA) or FITC conjugated CD44 or CD9 (BD Biosciences, San Jose, CA, USA) following the manufacturer's instructions. FITC non-immune isotypic IgG were used as a control. MSC EV were labelled with PKH26 to separate out EV from protein debris. To detect CD44 or CD9 on MSC EV, a BD FACSAria™ Fusion Special Order (SORP) cell sorter (BD Biosciences) with 100 nm nozzle and ND filter 1 was used. The threshold was set on the

SSC 200. Collected data were analyzed by Diva software (BD Biosciences). For fluorescence detection, we used a 586/15 band pass filter for PKH26 and 525/50 band pass filter for CD9, CD44 and their IgG controls. An unstained sample was used to detect auto-fluorescence and set the photomultiplier for all the considered channels. The instrument was rinsed with particle-free rinse solution before running samples and between each sample to eliminate the background. Standard silica beads (Apogee Mix for Flow Cytometer, Apogee Flow Systems Ltd, Hemel Hempstead, England), with a similar refractive index of vesicles, were used as internal size standards and to determine the gate for analysis.

Models and Assessment of Acute Lung Injury

C57BL/6 male mice (10–12 wks old, ~25 g; Jackson Laboratory, Bar Harbor, ME) were used in all experiments. The Institutional Animal Care and Use Committee at the University of California, San Francisco, approved all experimental protocols. The mice were first anesthetized with ketamine (90 mg/kg) and xylazine (10 mg/kg) (i.p.).

E.coli Endotoxin-Induced Acute Lung Injury.—Acute lung injury was induced by the intra-tracheal (IT) instillation of a nonlethal dose of endotoxin from *E.coli* O111: B4 (Sigma-Aldrich, St. Louis, MO) at 4 mg/kg; MSC (750,000 cells per mice) were given simultaneously as treatment. PBS was used as the carrier control and NHLF as a cellular control (750,000 cells per mouse). In separate experiments, MK-571 (Cayman Chemical, Ann Arbor, MI), a nonspecific inhibitor of MRP1, was instilled (i.v.) after endotoxin instillation at doses of 15, 35, or 50 mg/kg. Mice were sacrificed at 12, 24 or 48 h. MK-571 is both a leukotriene D_4 antagonist and MRP1 inhibitor (38,39).

E.coli Pneumonia.—Acute lung injury was induced by the IT instillation of *E.coli* K1 strain (1.5×10^6 colony forming units [cfu]). Four h later, MSC EV were injected IV with 90 μl of MSC EV per mouse (1×10^{10} particles). NHLF EV was used as a negative control. In separate experiments, in addition to MSC EV treatment, LY293111 (Cayman Chemical), an inhibitor of LTB_4 receptor1, was instilled (i.p.) at a dose of 18 mg/kg. In additional experiments, Reversan (Sigma-Aldrich), a specific inhibitor of both MRP1 and MDR1, was instilled (i.p.) after *E.coli* instillation at a dose of 40 mg/kg. Mice were sacrificed at 24 or 28 h.

At the end of the experiment, bronchoalveolar lavage fluid (BALF) from the lungs were collected for assessment of leukocyte counts, cytokine levels, bacterial load, protein levels, and histology. Total WBC count and differential were obtained using the Hemavet HV950FS (Drew Scientific, Miami Lakes, FL). Mouse macrophage inflammatory protein-2 (MIP-2), neutrophil chemokine (KC), TNF-α, LTB_4 and PGE_2 were measured in the BALF using ELISA kits (R&D Systems, Minneapolis, MN). The total protein concentration in BALF was measured with a BCA Protein Assay Kit (Pierce, Thermo Scientific, Wilmington, DE). CysLTs were measured with Amersham Leukotriene $C_4/D_4/E_4$ Biotrak Enzyme immunoassay (EIA) System (GE healthcare life science, Buckinghamshire, UK). For histologic analysis, the mouse lungs from each group were fixed in 4% paraformaldehyde and embedded in paraffin, cut into 5 μm sections, and stained with H&E.

miR-145 Mimic and Antagomir Experiments

To assess the role of miR-145 within MSC EV, we used a chemically synthesized antagomir of miR-145 (has-miR-145–5p, Thermo Fisher Scientific, Waltham, MA) and its negative control (mirVana ™ miRNA inhibitor Negative control #1, Thermo Fisher Scientific) for inhibition experiments. Lipofectamine RNAiMAX Transfection Reagent (Thermo Fisher Scientific Life Technology) was used to transfect miR-145 antagomir into MSC EV. We followed the manufacturer's instruction with modification (27). Briefly, MSC EV were incubated with Lipofectamine ™ RNAiMAX prepared miR-145 antagomir or antagomir negative control according to the protocol. The mixture was then incubated at 37 °C for 24 h followed by ultracentrifugation to pellet the transfected MSC EV. Residual antagomir or antagomir control was removed by washing the MSC EV with PBS. Antagomir transfected MSC EV were then co-cultured with Raw267.4 cells. Raw267.4 cells were seeded in 6-well plates and treated with LPS (100 ng/ml) and 90 μl of MSC EV (1×10^{10} particles), pre-transfected with miR-145 antagomir or a negative control.

We also used a chemically synthesized miR-145 mimic (has-miR-145–5p, Thermo Fisher Scientific) and its negative control (mirVana ™ miRNA mimic Negative control #1, Thermo Fisher Scientific) for agonist experiments. Briefly, miR-145 mimic was transfected to Raw264.7 cells with Lipofectamine RNAiMAX Transfection Reagent at 37 °C for 24 h.

Multidrug Resistance Assay

A fluoroimetric multi drug resistance (MDR) assay kit (Abcam, Cambridge, UK) was used to determine MRP1 activity. Mouse Raw264.7 cells (Sigma-Aldrich) were seeded into 96-well flat clear-bottom black-wall microplates and incubated for 24 h with or without stimulation with LPS (100 ng/ml). Cells were then treated with MSC CM, MSC CM with EV removed (CM supernatant), MSC EV (at doses of 2.5, 5, and 10 μl, equivalent to 3, 6, and 12 $\times10^{8}$ particles of MSC EV), MK-571: 1 μl (0.001 mM) and 2 μl (0.002 mM), or MSC EV transfected with miR-145 antagomir or its negative control. For miR-145 agonist experiments, Raw267.4 cells were pretreated with miR-145 mimic or its negative control. One hundred μl of MDR dye solution was added to each well and incubated at 37 °C for 2 h in the dark. Intracellular fluorescence intensity, as an indicator of MDR pump activity after co-incubation, was measured with a FLUOstar OPTIMA fluorescent plate reader (BMG Labtech, Cary, NC) at an excitation wavelength of 490 nm and an emission wavelength of 525 nm.

E.coli Bacteria Quantification

Bacterial growth in the BALF following *E.coli* pneumonia or in the supernatants of primary cultures of human monocytes exposed to *E.coli* bacteria with or without MSC EV was quantitated by counting CFU. The samples were cultured on LB agar plate (TEKnova, Hollister, California) overnight at 37 °C. Individual colonies (CFU) were then counted.

Phagocytosis of GFP Labelled E.coli Bacteria by Raw267.4 Cells

Raw267.4 cells were seeded in 6 well plate and treated with miR-145 mimic or its negative control and LPS for 24 h. After washing, cells were incubated with GFP labelled *E.coli* (1×107 CFU/well, (ATCC® 25922GFP™)) for 90 min. After washing, intracellular

fluorescence intensity was measured with a FLUOstar OPTIMA fluorescent plate reader following lysis of the cells.

MRP1 Western Blot Analyses

Human blood monocytes were isolated from healthy donors and cultured and stimulated with LPS with or without MSC EV. Cells were lysed with PLC lysis buffer plus protease inhibitor mixture (Sigma-Aldrich). Total proteins were separated out by SDS-PAGE and then transferred to PVDF membranes (Pall Corp, Ann Arbor, MI). Membranes were blocked in 3% BSA for 45 min at room temperature and then incubated with primary antibody solution overnight at 4 °C. Membranes were washed and then incubated with peroxidase-conjugated secondary antibodies (Jackson ImmunoResearch, West Grove, PA). Immunoblots were developed using SuperSignal West Dura Extended Duration Substrate (Thermo Scientific), and the signal was detected using a Gel Logic 2200 Imaging System (Eastman Kodak Co.) run on Carestream Imaging Software (Carestream Health, Rochester, NY). Antibodies used were MRP1 (0.5 μg/ml, Abcam) and actin (0.1 μg/ml, A2066, Sigma-Aldrich).

RNA Isolation and RT-PCR

Total RNA was isolated from MSC EV using the RNeasyMini Kit (Qiagen Sciences, Germantown, MD). After isolation, RNA samples were treated with DNase I for 60 min at room temperature. The quality of the RNA was assessed with the NanoDrop ND-1000 UV-Vis Spectrophotometer (NanoDrop Technologies, Wilmington, DE, USA) according to the manufacturer's instructions. The primers used for RT-PCR were human Ang-1 and human KGF (SABiosciences, Qiagen, Valencia, CA). The RT-PCR assays were conducted using the SuperScript III One-Step RT-PCR protocol as described by the manufacturer (SABiosciences, Qiagen). For cDNA amplification, an initial reverse transcription step (52°C for 30 min) was followed by a denaturing step (94°C for 2 min) and then by 40 cycles of denaturing (94°C for 20 s), annealing (60°C for 30 s), and extending (68°C for 30 s), followed by 5 min at 72°C for elongation. *GAPDH* gene amplification was used as an internal control. The amplified DNA products were run on a 1.4% agarose gel, and bands were visualized with the use of ethidium bromide.

Quantitative Real-Time PCR

Total RNA was isolated using the miRNeasy Mini Kit (QIAGEN Sciences, Germantown, MD). Total mRNA concentrations were determined with a ND-1000 (NanoDrop/Thermo Fisher Scientific). For MRP1 and GAPDH expression, mRNA was reverse-transcribed to cDNA using the High Capacity RNA-to-cDNA kit (Applied Biosystems, Foster City, CA). The primers MRP1 (Mm00456156_m1), MMP-9 (Mm00442991_m1) and GAPDH (Mm99999915_g1) were purchased from Thermo Fisher Scientific (Waltham, MA, USA). TaqMan Fast Advanced Master Mix (Applied Biosystems) was used in qRT-PCR experiments, and qRT-PCR was performed using the StepOnePlusTM System (Applied Biosystems). PCR activation at 95 °C for 20 s was followed by 40 cycles of 1 s at 95 °C and 20 s at 60 °C. For miR-145 and U6 expression, miRNA was reverse-transcribed to cDNA using the TaqMan MicroRNA Reverse Transcription Kit (Applied Biosystems, Foster City, CA). The primers miR-145 (has-miR-145–5p) and U6 (U6 snRNA) were purchased from

Thermo Fisher Scientific (Waltham, MA, USA). TaqMan Universal Master Mix II (Applied Biosystems) was used in qPCR experiments, and qPCR was performed using the StepOnePlusTM System (Applied Biosystems). PCR activation at 95 °C for 10 min was followed by 40 cycles of 15 s at 95 °C and 60 s at 60 °C. GAPDH and U6 were used as mRNA and microRNA internal references respectively.

The average Ct value of two technical replicates was used in all calculations with specific gene expression assays. The average Ct value of the internal controls GAPDH or U6 were used to calculate ΔCt values for the array samples as this combination of reference genes displayed the lowest standard deviation among groups. GAPDH or U6 alone was used to calculate ΔCt values for specific gene expression assays. The initial data analysis was performed using the $2^{-\Delta\Delta}$Ct method.

LTA_4H *Quantification*

MSC EV were transfected with miR-145 antagomir or negative control for 24 h. Ninety μl (1×10^{10} particles) MSC EV was then co-cultured with RAW267.4 cells in 6-well plates stimulated with LPS (100 ng/ml). LTA_4H and MMP-9 levels in the supernatant were measured with an ELISA (USCN Life Science, Hubei, PRC and R&D Systems, Minneapolis, MN). Cells were collected and processed for real-time PCR for MMP-9 expression.

Statistics

Data were presented as the mean ± SD or median with interquartile range (IQR). Shapiro-Wilk normality test and Kolmogorov-Smirnov test with Dallal-Wilkinson-Lillie for *p* value were used to determine if the values were from a Gaussian distribution. Comparisons between two groups were made using Student's *t*-test (for parametric data) or the Mann–Whitney *U*- test (for non-parametric data). Comparisons between more than two groups were made using 1-way ANOVA with the Bonferroni's correction (for parametric data) or Kruskal–Wallis test with Dunn's correction (for non-parametric data) for multiple comparison testing. A p value < 0.05 was considered statistically significant. All statistical analysis was performed using GraphPad Prism 6.0 software (GraphPad, Inc., San Diego, CA).

Results

Isolation and Characterization of MSC EV

EV were isolated from the conditioned medium of human bone marrow derived MSC. Human MSC were serum starved for 48 h. The viability of serum starved MSC before EV isolation was > 95% (trypan blue exclusion). Conditioned medium was collected, and MSC EV were isolated using ultracentrifugation as previously described (23,24,37). Scanning electron microscopy showed that the isolation technique yielded homogeneous population of spheroid particles the size of approximately 200 nm (Supplemental Fig. 1A). NanoSight analysis from multiple samples showed MSC EV mean size was 227 ± 25 nm, and mode size was 146 ± 22 nm with a concentration of $1.2 \pm 0.2 \times10^{11}$ particles per ml or $1.2 \pm 0.2 \times10^{8}$ particles per μl (Supplemental Fig. 1B).

Total protein and RNA content of MSC EV were 1.1 ± 0.3 μg (n = 5) and 0.9 ± 0.4 ng per μl EV (n = 5) respectively (Supplemental Fig. 1C), which falls into a range of concentrations found in previous studies (23,24,37). By RT-PCR, MSC EV expressed mRNA for angiopoietin 1 and keratinocyte growth factor which are soluble factors secreted by MSC and known to participate in the therapeutic effects of MSC in acute lung injury (Supplemental Fig. 1D) (23,24). Based on previous dose-response experiments (23), 90 μl MSC EV per mice (1×10^{10} particles) was the optimal dose used in the *in vivo* experiments.

CD9 is a known marker on exosomes, and CD44 is a key plasma membrane receptor involved in MSC trafficking (40); we previously demonstrated that MSC EV expressed CD44 with Western blot analyses (23). For flow cytometry, we labelled MSC EV with PKH26 to quantify only membrane bound vesicles and exclude protein debris. Flow cytometry analyses showed > 73% (74 ± 8) of MSC EV expressed CD44 and < 0.3% (0.3 ± 0.4) expressed CD9 (Supplemental Fig. 1E), suggesting that the majority of EV were microvesicles. Furthermore, similar to their parent MSC, MSC EV expressed CD44 on their surface, which was instrumental in incorporating MSC EV into target cells in previous studies.

MSC EV Decreased MRP1 Protein levels in LPS Stimulated Human Monocytes

To determine whether or not MSC EV suppressed MRP1 expression and activity, we cultured normal adult human blood monocytes stimulated with LPS with or without MSC EV. Western blot analyses demonstrated a 190 kDa band corresponding to MRP1 protein using a monoclonal antibody specific for MRP1 (no cross-reaction with P-glycoprotein) (Fig. 2A). Compared to controls, MSC EV suppressed MRP1 protein levels in human monocytes, which was associated with increased phagocytosis of *E.coli* bacteria (Fig. 2B).

MRP1 Functional Assay

To determine if MSC EV suppressed MRP1 pump function, a fluoroimetric MDR assay kit was used. P-glycoprotein (Pgp, MDR1) and MRP1 are members of the ABC transporter family; they are cell membrane proteins and function as ATP dependent drug efflux pumps. This MDR assay kit uses a fluorescent MDR indicator dye to assay these two pump activities. The hydrophobic fluorescent dye rapidly penetrates cell membranes and becomes trapped in cells. In the MDR1 and/or MRP1-expressing cells, this dye is extruded by MDR transporters, thus decreasing cellular fluorescence intensity. However, when MDR1 and/or MRP1 pump-activity are suppressed, their intracellular dye cannot be pumped out, thus increasing intracellular fluorescence intensity. A mouse macrophage cell line Raw267.4, which highly expresses MRP1 upon stimulation with LPS, was used in this assay. We cultured Raw267.4, stimulated with LPS, with or without MSC conditioned medium (CM) or MSC EV. Similar to MRP1 protein expression, administration of MSC CM down-regulated MRP1 pump activity on Raw267.4 cells as evidenced by increased intracellular fluorescence intensity compared to PBS (Fig. 2C). MSC CM which contains EV had a stronger effect on suppressing MRP1 pump activity compared to CM with EV removed (named CM supernatant) by ultracentrifugation but containing soluble factors (Fig. 2D). MSC EV also inhibited MRP1 activity in a dose-dependent manner (Fig. 2E) at dosages of 2.5, 5, and 10 μl, (equivalent to 3, 6, and 12 $\times10^{8}$ particles of MSC EV). We then compared

MSC EV to MK-571, a nonspecific MRP1 inhibitor, in the MDR pump assay. MSC EV (5 μl, equals 6×10^8 particles) had a similar effect on inhibiting MDR pump activity as MK-571 (2 μl, equals 0.002 mM) (Fig. 2F). We also studied the role of miR-145 by transfection of EV with miR-145 antagomir (synthetic miR inhibitor that degrades miR-145). Similar to EV in Fig. 2E **and** F, EV transfected with miR negative control showed increased fluorescent intensity (Fig. 2G). However, EV transfected with miR-145 antagomir abolished this effect. In contrast, transfection of Raw264.7 cells with a miR-145 mimic (synthetic miR-145) showed increased fluorescent intensity compared to that of negative control (Fig. 2H).

MSC or MSC EV Treatment Increased LTB_4 Levels in BALF of Mice with Acute Lung Injury

We measured LTB_4 levels in mice with acute lung injury from LPS or *E.coli* bacteria. Baseline level of LTB_4 in BALF was low but increased with stimulation with LPS or *E.coli* bacteria (data not shown). MSC or MSC EV treatment following acute lung injury resulted in significantly higher LTB_4 level in BALF compared to PBS treatment (Fig. 3). The level of LTB_4 was significantly higher in MSC or MSC EV treatment groups compared with NHLF or NHLF EV groups, which was used as cellular controls. LTB_4 level was increased in the plasma after MSC treatment (Fig. 3A). We also measured CysLTs ($LTC_4D_4E_4$) level in BALF in mice with acute lung injury from LPS or *E.coli* bacteria. There were no significant differences in CysLTs level in all groups.

Prostaglandin E_2 (PGE_2)/LTB_4 Ratio in Acute Lung Injury Mice Treated with MSC or MSC EV

Similar to LTB_4, baseline level of PGE_2 in BALF was low but increased with stimulation with LPS or *E.coli* bacteria. Unlike LTB_4, the level of PGE_2, a lipid mediator with anti-inflammatory properties known to be secreted by MSC, was unchanged in the BALF after MSC or MSC EV treatment compared to PBS treated mice injured with LPS or *E.coli* (data not shown), which is consistent with our previous study (41). However, the ratio of PGE_2 (ng/ml)/ LTB_4 (pg/ml) decreased with treatment with MSC or MSC EV (Supplemental Fig. 2A **and** B).

MRP1 Inhibitor Reduced Lung Injury

MK-571, a commonly used nonspecific MRP1 inhibitor, was administered in LPS-induced acute lung injury in mice to corroborate the importance of MRP1 activity during lung injury. Compared to PBS treated LPS injured mice, MK-571 administration significantly reduced WBC and neutrophil counts (Fig. 4A) and pro-inflammatory cytokines (TNFα, MIP-2, and KC) levels (Fig. 4B) and demonstrated a trend towards decreased protein levels in BALF (Fig. 4C). These results suggested that MRP1 inhibition by MK-571 had significant anti-inflammatory properties.

LTB_4 level in BALF was barely detected in all groups at 12 h, while higher levels of LTB_4 were observed only in MK-571 treated mice compared to PBS treated LPS injured mice at 24 h (Fig. 4D). In contrast, CysLTs levels in all groups were higher at 12 h than that at 24 h (Fig. 4E). Compared to PBS treated LPS injured mice, MK-571 administration significantly reduced CysLTs production at 12 h (Fig. 4E). These results suggested that MK-571 may

inhibit MRP1-mediated transport of LTC_4 and thus reduce CysLTs and increase LTB_4 production. CysLTs are pro-inflammatory lipids which can increase vascular permeability.

A more selective MRP1 inhibitor, Reversan, was used in mice with *E.coli* pneumonia. Administration of Reversan significantly reduced the bacterial CFU counts (Fig. 5A) and the total WBC and neutrophil counts (Fig. 5B) in the BALF following *E.coli* pneumonia.

Administration of MRP1 inhibitors (MK-571 and Reversan) behaved in a similar manner as MSC or MSC EV in mice with acute lung injury, suggesting that MSC or MSC EV may share a common mechanism with MK-571 or Reversan (i.e., inhibition of MRP1 activity). Similar to MSC or MSC EV treatment, PGE_2/LTB_4 ratio was lower in MK-571 treated mice although not statistically significant (Supplemental Fig. 2C).

LY293111, a LTB_4 BLT1 Antagonist, Inhibited the Effect of MSC EV on E.coli Bacterial Levels

To determine if the antimicrobial effect of MSC EV was mediated by LTB_4, LY293111, a specific antagonist of LTB_4 BLT1, was administered in mice with *E.coli* pneumonia treated with MSC EV.

Mice were infected with *E.coli* bacteria, and, 4 h later, MSC EV alone or together with LY293111 were administrated to the mice. Treatment with MSC EV significantly reduced the bacterial CFU counts in the BALF compared to PBS treatment. However, administration of MSC EV together with LY293111 abolished this effect (Fig. 5C). MSC EV treatment also reduced the total inflammatory cells and levels of TNFα and MIP-2 in the BALF, which was abolished by LY293111 co-treatment (Fig. 5D **and** E).

MiR-145 Regulates the Expression of MRP1

We next determined whether MSC or MSC EV down-regulated MRP1 activity through the transfer of miR-145. We first co-cultured LPS stimulated Raw267.4 cells with MSC pretreated with or without miR-145 antagomir. Real-time PCR showed that *MRP1* mRNA expression decreased with MSC treatment. However, the effect of MSC on MRP1 suppression was abolished when MSC was pretreated with miR-145 antagomir (Fig. 6A).

To confirm the effect of MSC EV on MRP1 suppression was due to transfer of miR-145 by MSC EV, we transfected MSC EV with miR-145 antagomir or negative control prior to co-culture. MiR-145 level in the EV was reduced by miR-145 antagomir (Fig. 6B). More importantly, compared to PBS treatment, MSC EV transfected with negative control significantly decreased MRP1 expression, while MSC EV with miR-145 knockdown (miR-145 antagomir) failed to do so (Fig. 6C). These results suggested that the transfer of miR-145 from MSC EV to target Raw267.4 cells contributed to the suppression of *MRP1* expression.

We then determined if increased miR-145 expression in Raw264.7 cell regulated the expression of *MRP1*. Raw267.4 cells were transfected with miR-145 mimic or negative control. Real-time PCR showed that miR-145 level was significantly increased by miR-145 mimic (Fig. 6D), and MRP1 expression decreased accordingly (Fig. 6E). Our results

suggested that *Mrp1* was the target of miR-145, and miR-145 negatively regulated *MRP1* expression.

MiR-145 Mimic Increased the Phagocytosis of E.coli Bacteria by Raw267.4 Cells

We examined whether increased miR-145 expression increased the phagocytic capacity of Raw267.4 cells against GFP labelled *E.coli* bacteria. Raw267.4 cells transfected with miR-145 mimic showed increased fluorescent intensity compared to that of mimic negative control (Fig. 6F **and** G).

Knockdown of miR-145 in MSC EV Inhibited the Effect of MSC EV on E.coli Bacterial Levels

We next determined whether miR-145 antagomir treatment would have an impact on *in vivo* antimicrobial activity of MSC EV. MSC EV pretreated with either miR-145 antagomir or negative control was administrated to *E.coli* pneumonia injured mice. As shown in Fig. 7A, intra-tracheal administration of *E.coli* bacteria resulted in a significant bacterial load at 28 h in the BALF which was reduced with MSC EV therapy. However, antagomir pre-treatment of MSC EV increased CFU counts more than threefold over MSC EV negative control treatment. In addition, the beneficial effects of MSC EV treatment on reducing the total WBC and neutrophils counts and levels of TNFα and protein concentration in the BALF was abolished by miR-145 antagomir treatment (Fig. 7B - D). Thus, knockdown of miR-145 in MSC EV significantly decreased the *in vivo* antimicrobial and anti-inflammatory effect of MSC EV. Our results suggested that miR-145 level was inversely correlated with MRP1 at the levels of mRNA (Fig. 6, A - E), protein function (Fig. 2, G and H), and phagocytosis (Fig. 6, F **and** G). The therapeutic activity of MSC EV in acute lung injury were mediated via miR-145 (Fig. 7) by down-regulating MRP1 function.

Effect of MSC EV on Extracellular LTA_4H and MMP-9 Expression

Extracellular LTA_4H can reduce inflammation by degrading PGP which is generated from ECM collagen via enzymes such as MMP-9. We measured LTA_4H and MMP-9 protein levels in the supernatant of injured Raw267.4 cells co-incubated with MSC EV (pretreated with miR-145 antagomir or negative control). LTA_4H was elevated at 14 h in MSC EV negative control treatment group compared with PBS (Supplemental Fig. 3A). MMP-9 protein level was found to be elevated in all three groups over 24 h (data not shown). However, at 24 h, treatment with MSC EV negative control significantly reduced *MMP-9* mRNA expression and demonstrated a trend towards reduced MMP-9 protein expression (Supplemental Fig. 3B **and** C). The effect of increasing LTA_4H and decreasing *MMP-9* expression were abolished when MSC EV was pretreated with miR-145 antagomir (Supplemental Fig. 3A - C).

Discussion

Our study demonstrated that: (1) MSC and MSC EV administration led to significantly higher LTB_4 levels in the BALF in both LPS-induced acute lung injury and *E.coli* pneumonia in mice (Fig. 3); (2) MSC EV had significant antimicrobial activity in mice with *E.coli* pneumonia, which was mediated in part by LTB_4 activity through BLT1 receptor (Fig.

5C) and which was abolished by the knockdown of miR-145 (Fig. 7A); (3) MSC EV treatment decreased MRP1 mRNA expression (Fig. 6C), protein levels (Fig. 2A), and pump activity (Fig. 2E). These effects were abolished by knockdown of miR-145. (Fig. 6C, 2G); (4) Similar to MSC EV, administration of MRP1 inhibitors (MK-571 or Reversan) decreased the influx of inflammatory cells (Fig. 4A, 5B), bacteria (Fig. 5A), LTC_4, (Fig. 4E) and subsequently increased LTB_4 levels (Fig. 4D) in mice with acute lung injury; (5) Similar to MSC EV, Raw267.4 cells transfected with the miR145 mimic had decreased MRP1 mRNA expression (Fig. 6E), MRP1 pump activity (Fig. 2H), and enhanced phagocytosis activity against *E.coli* bacteria (Fig. 6F). Taken together, our study revealed for the first time, to our knowledge, that MSC EV suppressed MRP1 expression through transfer of miR-145, which resulted in reduced extracellular level of LTC_4 and enhanced LTB_4 production. Increased LTB_4 levels then mediated increased antimicrobial activity through LTB_4/BLT1 signaling (Fig. 1).

We and other investigators have demonstrated the therapeutic effects of MSC or MSC EV in acute lung injury models of inflammation and infection (23-26). We showed that MSC EV reduced the total bacterial load in both mice (23) and *ex vivo* perfused human lung (26) injured with *E.coli* pneumonia. However, the mechanisms underlying the antimicrobial activity of MSC EV remain largely unknown. Recent studies have demonstrated significant antimicrobial effects of LTB_4 in pneumonia and sepsis (9-12). These studies provided the biological rationale for our hypothesis that the antimicrobial effect of MSC or MSC EV in acute lung injury were in part through increased LTB_4 activity. High level of LTB_4 in BALF was detected in both MSC EV treated *E.coli* pneumonia mice and MSC treated LPS-induced acute lung injury mice (Fig. 3). MSC EV treatment also showed improved bacterial clearance in *E.coli* pneumonia mice. However, this effect was abrogated by co-treatment with LY293111 (Fig. 5C), suggesting that the LTB_4/BLT1 axis was a key determinant in the antimicrobial effect of MSC EV.

To determine if MSC or MSC EV reduced MRP1 expression and thus increased LTB_4 levels, we first studied the effect of MSC EV on MRP1 protein expression and function *in vitro*. Western blot analyses showed that MRP1 expression on LPS-stimulated monocytes was reduced after MSC EV treatment (Fig. 2A) which was associated with increased antimicrobial activity (Fig. 2B). MDR assay showed that MSC CM or isolated MSC EV increased intracellular fluorescence intensity in LPS-stimulated Raw267.4 cells, which resulted from decreased MRP1 pump-activity (Fig. 2, C - E).

We then administered MK-571 to mice with LPS induced acute lung injury to explore whether the inhibition of MRP1 affected the production of LTs. Similar to MSC EV, administration of MK-571 inhibited the influx of inflammatory cells and reduced pro-inflammatory cytokines in BALF in a dose-dependent manner (Fig. 4A **and** B). Efflux of LTC_4 was impaired after MK-571 treatment as indicated by decreased CysLTs levels at 12 h (Fig. 4E), which was associated with an increase in LTB_4 levels at 24 h (Fig. 4D). A more selective MRP1 inhibitor, Reversan, was used in mice with *E.coli* pneumonia. Similar to MSC EV, Reversan significantly reduced the bacterial CFU counts and the infiltration of inflammatory cells in the BALF (Fig. 5A **and** B). Administration of MK-571 or Reversan behaved in a similar fashion as MSC or MSC EV, suggesting that they may share a common

mechanism (i.e., the inhibition of MRP1). However, compared to MK-571, MSC EV treatment resulted in significantly higher LTB_4 levels in either LPS-injured or *E.coli* pneumonia in mice (Fig. 3, 4D). This suggested that MSC or MSC EV may have a stronger effect on MRP1 suppression than MK-571 or there were other mechanisms in which MSC or MSC EV may enhance the production of LTB_4. The MDR pump assay showed that MSC EV had a similar effect as MK-571 on inhibiting MDR pump activity (Fig. 2F). Thus, there might be some other signals involved in LTB_4 production. We previously demonstrated that MSC itself secreted LL-37 (42), a peptide with broad-spectrum bactericidal activity. LTB_4 is known to interact with LL-37. LTB_4 can trigger the release of LL-37 in a BLT1 dependent way. Meanwhile, LL-37 can cause the translocation of the enzyme 5-lipoxygenase to the peri-nuclear membrane which can promote the production of LTB_4. LL-37 can also enhance LTB_4-induced phagocytosis (43,44). In the current study, MSC EV suppressed MRP1 activity was associated with enhanced production of LTB_4. LTB_4 may work with LL-37 in a synergistic fashion to suppress inflammation and decrease bacteria growth (Fig. 1).

Although LTs are secreted predominantly by leukocytes, treatment with MSC, MSC EV, and MK-571 reduced the influx of inflammatory cells (23-26,45), which was associated with increased LTB_4 levels in the BALF (Fig. 3 **and** Fig. 4). There are several possibilities why LTB_4 level can be high with low leukocyte numbers. Studies have showed that MSC can inhibit neutrophil apoptosis, prolong leukocyte survival, and enhance their function (46,47), possibly leading to enhanced antimicrobial activity, decreasing the trafficking of immune cells to the injured alveolus. In addition, the actual conversion to LTB_4 may result from trans-cellular biosynthesis. The synthesis of LTB_4 requires two steps from AA via individual enzymes. Once LTA_4 is produced by inflammatory cells, it can be transferred to LTA_4H containing cells to generate LTB_4 or LTC_4S containing cells to generate LTC_4 (48-52), possibly reducing the overall production of LTB_4 by neutrophils. In addition, AA can also be transferred between cells (52-54).

MSC and MSC EV showed similar protective effects on acute lung injury both *in vivo* and *in vitro* by decreasing inflammation and lung permeability and enhancing antimicrobial activity (23-26,45). To understand the mechanism, we studied the activity of intra-cellular or vesicular miR-145 as it was found in both MSC and MSC EV (29,31), and it was previously shown to regulate MRP1 expression (33,34). By qPCR and pump activity assay, MRP1 mRNA expression and MRP1pump function on LPS-stimulated Raw267.4 cells were down-regulated with MSC EV treatment, and this effect was eliminated by knockdown of miR-145 (Fig. 6C, 2G). MSC EV treatment improved bacterial clearance in *E.coli* pneumonia mice, and this effect was abrogated by miR-145 knockdown (Fig. 7A). In corroboration, Raw267.4 cells, transfected with miR145 mimic, had decreased MRP1 mRNA expression (Fig. 6E), decreased pump activity (Fig. 2H), and improved bacterial clearance (Fig. 6F). Our data suggested that miR-145 is a key regulator of MRP1 expression and function, in agreement with recent studies (33,34) that miR-145 directly regulated MRP1 expression by increasing MRP1 mRNA degradation by targeting its 3'- untranslated region (UTR) of the *Mrp1* gene.

Extracellular LTA_4H was reported to help facilitate the resolution of inflammation in various pulmonary disorders through the degradation of PGP, which is generated from ECM collagen via MMP-9 (18,20-22). We previously showed that MMP-9 level in the BAL fluid

was significantly reduced in MSC treated acute lung injury mice compared to control (25). In the current study, we showed that MSC EV treatment led to increased LTA_4H levels and decreased MMP-9 mRNA expression. These effects were miR-145 dependent (Supplemental Fig. 3, A - C). Increased extracellular LTA_4H and reduced MMP-9 may be involved in the anti-inflammatory effect of MSC EV as well (Fig. 1).

AA can also be metabolized to prostaglandin H_2 (PGH_2) through the enzyme cyclooxygenase, which is then converted to PGE_2 and transported outside via multidrug resistance protein 4. Inhibition of PGE_2 may decrease bacterial growth. Recent study showed the protective effect of adipose tissue-derived MSC against *P. aeruginosa* pneumonia was in part by inhibiting PGE_2, which subsequently increased macrophage phagocytosis (55). In our study, PGE_2 level did not change after MSC EV treatment in *E.coli* pneumonia in mice, suggesting the therapeutic effect may not be attributed to reduced PGE_2 level alone. It remains controversial whether PGE_2 is beneficial or plays a negative role in infection (55-58). Previous studies showed that LTB_4 can enhance, whereas, PGE_2 can inhibit phagocytosis of bacteria by alveolar macrophage (11,59,60) via cyclic AMP (cAMP) (11,59). In addition, other studies have shown that increased PGE_2/LTB_4 ratio was associated with increased *L. infantum* infection (61). MSC and PGs can both affect ABC transport protein expression and function as well (62-65). For example, PGE_2 can induce *MRP1* mRNA expression in human bronchial epithelium (63). Thus, the ratio between PGE_2 and LTB_4 may reflect MRP1 levels and overall antimicrobial activity. Our data showed that decreased PGE_2/LTB_4 ratio was associated with the therapeutic effects of MSC or MSC EV (Supplemental Fig. 2). The importance of PGE_2 and LTB_4 on inflammation and infection with MSC therapy needs further study.

There are some limitations to the current study which requires further study: 1) We cannot exclude the possibility that other target gene(s) besides *Mrp1* might be involved in the therapeutic effect of MSC EV via miR-145. Recently, Shinohara and his colleagues showed that miR-145 within cancer EV can target HDAC11 and promote IL-10 expression and M2 macrophage polarization (66). Our previous studies showed that MSC or MSC EV administration can upregulate IL-10 mRNA or protein expression (23,41). Whether there is some connection between MSC EV miR-145 and IL-10 production will need to be investigated; 2) LY293111, the antagonist of BLT1, only partially reduced the antimicrobial and anti-inflammatory activity of MSC EV (Fig. 5, C-E), suggesting other leukotriene derived factors may be involved in the anti-inflammatory effect. We and others have recently found that human MSCs promoted the resolution of LPS induced acute lung injury or following polymicrobial sepsis in mice in part through the secretion of specialized pro-resolving lipid mediators such as lipoxin A_4 or resolvins (67,68). Lipoxin A_4 is derived directly from LTA_4 and has anti-inflammatory properties in both sterile and infectious animal models of injury (67,69). Studies are on-going whether EV derived from MSCs can generate specialized pro-resolving lipid mediators, similar to the parent cells, and what role they have if any in the overall therapeutic effect; 3) The MDR pump assay assessed both MDR1 and MRP1 function, not MRP1 alone. The effect of MSC EV on MDR1 activity in the overall therapeutic effect will need to be explored.

In summary, MSC EV suppressed MRP1 expression in part through the transfer of miR-145, which resulted in enhanced LTB_4 production and subsequently increased bacterial phagocytosis through LTB_4/BLT1 signaling. This represents a previously undescribed mechanism underlying the antimicrobial activity of MSC or MSC EV.

Supplementary Material

Refer to Web version on PubMed Central for supplementary material.

Acknowledgements

We thank Dr. Airan Liu for help with MSC EV analyses, Dr. Hyungsun Lim for assistance with the animal experiments, and Dr. Stephane Gennai for assistance with the preparation of MSC EV.

This study was supported by Grant HL-113022 from National Heart, Lung and Blood Institute at National Institutes of Health (to J.W.L.).

Abbreviations used in this article:

BALF	bronchoalveolar lavage fluid
CysLTs	cysteinyl leukotrienes
ECM	extracellular matrix
E.coli	Escherichia coli
LTA_4	leukotriene A_4
LTA_4H	LTA_4 hydrolase
LTB_4	leukotriene B_4
LTC_4	leukotriene C_4
LTC_4S	LTC_4 synthase
LTD_4	leukotriene D_4
MSC	mesenchymal stem cell
MSC CM	MSC conditioned medium
MSC EV	MSC extracellular vesicle
MRP1	Multidrug-resistance associated protein 1
MDR1	multidrug resistance protein 1
miR	microRNA
MMP	matrix metalloproteinase
NHLF	Normal adult human lung fibroblast

PGE_2	prostaglandin E_2
PGP	proline-glycine-proline

REFERENCES

1. Keppler D 1992 Leukotrienes: biosynthesis, transport, inactivation, and analysis. Rev. Physiol. Biochem. Pharmacol. 121: 1–30. [PubMed: 1485071]
2. Sala A, Zarini S, and Bolla M. 1998 Leukotrienes: lipid bioeffectors of inflammatory reactions. Biochemistry (Mosc) 63: 84–92. [PubMed: 9526099]
3. Sharma JN, and Mohammed LA. 2006 The role of leukotrienes in the pathophysiology of inflammatory disorders: is there a case for revisiting leukotrienes as therapeutic targets? Inflammopharmacology 14: 10–16. [PubMed: 16835707]
4. Samuelsson B, Dahlen SE, Lindgren JA, Rouzer CA, and Serhan CN. 1987 Leukotrienes and lipoxins: structures, biosynthesis, and biological effects. Science 237: 1171–1176. [PubMed: 2820055]
5. Peters-Golden M, and Henderson WR Jr. 2007 Leukotrienes. N. Engl. J. Med. 357: 1841–1854. [PubMed: 17978293]
6. Funk CD 2005 Leukotriene modifiers as potential therapeutics for cardiovascular disease. Nat. Rev. Drug Discov. 4: 664–672. [PubMed: 16041318]
7. Wirth JJ, and Kierszenbaum F. 1985 Stimulatory effects of leukotriene B4 on macrophage association with and intracellular destruction of Trypanosoma cruzi. J. Immunol. 134: 1989–1993. [PubMed: 2857187]
8. Flamand L, Tremblay MJ, and Borgeat P. 2007 Leukotriene B4 triggers the in vitro and in vivo release of potent antimicrobial agents. J. Immunol. 178: 8036–8045. [PubMed: 17548641]
9. Schultz MJ, Wijnholds J, Peppelenbosch MP, Vervoordeldonk MJ, Speelman P, van Deventer SJ, Borst P, and van der Poll T. 2001 Mice lacking the multidrug resistance protein 1 are resistant to Streptococcus pneumoniae-induced pneumonia. J. Immunol. 166: 4059–4064. [PubMed: 11238654]
10. Mancuso P, Peters-Golden M, Goel D, Goldberg J, Brock TG, Greenwald-Yarnell M, and Myers MG Jr. 2011 Disruption of leptin receptor-STAT3 signaling enhances leukotriene production and pulmonary host defense against pneumococcal pneumonia. J. Immunol. 186: 1081–1090. [PubMed: 21148797]
11. Soares EM, Mason KL, Rogers LM, Serezani CH, Faccioli LH, and Aronoff DM. 2013 Leukotriene B4 enhances innate immune defense against the puerperal sepsis agent Streptococcus pyogenes. J. Immunol. 190: 1614–1622. [PubMed: 23325886]
12. Mancuso P, Lewis C, Serezani CH, Goel D, and Peters-Golden M. 2010 Intrapulmonary administration of leukotriene B4 enhances pulmonary host defense against pneumococcal pneumonia. Infect. Immun. 78: 2264–2271. [PubMed: 20231413]
13. Leier I, Jedlitschky G, Buchholz U, Cole SP, Deeley RG, and Keppler D. 1994 The MRP gene encodes an ATP-dependent export pump for leukotriene C4 and structurally related conjugates. J. Biol. Chem. 269: 27807–27810. [PubMed: 7961706]
14. Loe DW, Almquist KC, Deeley RG, and Cole SP. 1996 Multidrug resistance protein (MRP)-mediated transport of leukotriene C4 and chemotherapeutic agents in membrane vesicles. Demonstration of glutathione-dependent vincristine transport. J. Biol. Chem. 271: 9675–9682. [PubMed: 8621643]
15. Wijnholds J, Evers R, van Leusden MR, Mol CA, Zaman GJ, Mayer U, Beijnen JH, van der Valk M, Krimpenfort P, and Borst P. 1997 Increased sensitivity to anticancer drugs and decreased inflammatory response in mice lacking the multidrug resistance-associated protein. Nat. Med. 3: 1275–1279. [PubMed: 9359705]
16. Robbiani DF, Finch RA, Jager D, Muller WA, Sartorelli AC, and Randolph GJ. 2000 The leukotriene C(4) transporter MRP1 regulates CCL19 (MIP-3beta, ELC)-dependent mobilization of dendritic cells to lymph nodes. Cell 103: 757–768. [PubMed: 11114332]
17. Bakos E, and Homolya L. 2007 Portrait of multifaceted transporter, the multidrug resistance-associated protein 1 (MRP1/ABCC1). Pflugers Arch. 453: 621–641. [PubMed: 17187268]

18. Snelgrove RJ, Jackson PL, Hardison MT, Noerager BD, Kinloch A, Gaggar A, Shastry S, Rowe SM, Shim YM, Hussell T, and Blalock JE. 2010 A critical role for LTA4H in limiting chronic pulmonary neutrophilic inflammation. Science 330: 90–94. [PubMed: 20813919]

19. Gaggar A, Jackson PL, Noerager BD, O'Reilly PJ, McQuaid DB, Rowe SM, Clancy JP, and Blalock JE. 2008 A novel proteolytic cascade generates an extracellular matrix-derived chemoattractant in chronic neutrophilic inflammation. J. Immunol. 180: 5662–5669. [PubMed: 18390751]

20. Paige M, Wang K, Burdick M, Park S, Cha J, Jeffery E, Sherman N, and Shim YM. 2014 Role of leukotriene A4 hydrolase aminopeptidase in the pathogenesis of emphysema. J. Immunol. 192: 5059–5068. [PubMed: 24771855]

21. Akthar S, Patel DF, Beale RC, Peiro T, Xu X, Gaggar A, Jackson PL, Blalock JE, Lloyd CM, and Snelgrove RJ. 2015 Matrikines are key regulators in modulating the amplitude of lung inflammation in acute pulmonary infection. Nat. Commun. 6: 8423. [PubMed: 26400771]

22. Wells JM, O'Reilly PJ, Szul T, Sullivan DI, Handley G, Garrett C, McNicholas CM, Roda MA, Miller BE, Tal-Singer R, Gaggar A, Rennard SI, Jackson PL, and Blalock JE. 2014 An aberrant leukotriene A4 hydrolase-proline-glycine-proline pathway in the pathogenesis of chronic obstructive pulmonary disease. Am. J. Respir. Crit. Care Med. 190: 51–61. [PubMed: 24874071]

23. Monsel A, Zhu YG, Gennai S, Hao Q, Hu S, Rouby JJ, Rosenzwajg M, Matthay MA, and Lee JW. 2015 Therapeutic Effects of Human Mesenchymal Stem Cell-derived Microvesicles in Severe Pneumonia in Mice. Am. J. Respir. Crit. Care Med. 192: 324–336. [PubMed: 26067592]

24. Zhu YG, Feng XM, Abbott J, Fang XH, Hao Q, Monsel A, Qu JM, Matthay MA, and Lee JW. 2014 Human mesenchymal stem cell microvesicles for treatment of Escherichia coli endotoxin-induced acute lung injury in mice. Stem Cells 32: 116–125. [PubMed: 23939814]

25. Hao Q, Zhu YG, Monsel A, Gennai S, Lee T, Xu F, and Lee JW. 2015 Study of Bone Marrow and Embryonic Stem Cell-Derived Human Mesenchymal Stem Cells for Treatment of Escherichia coli Endotoxin-Induced Acute Lung Injury in Mice. Stem Cells Transl. Med. 4: 832–840. [PubMed: 25999518]

26. Lee JW, Krasnodembskaya A, McKenna DH, Song Y, Abbott J, and Matthay MA. 2013 Therapeutic effects of human mesenchymal stem cells in ex vivo human lungs injured with live bacteria. Am. J. Respir. Crit. Care Med. 187: 751–760. [PubMed: 23292883]

27. Fang S, Xu C, Zhang Y, Xue C, Yang C, Bi H, Qian X, Wu M, Ji K, Zhao Y, Wang Y, Liu H, and Xing X. 2016 Umbilical Cord-Derived Mesenchymal Stem Cell-Derived Exosomal MicroRNAs Suppress Myofibroblast Differentiation by Inhibiting the Transforming Growth Factor-beta/SMAD2 Pathway During Wound Healing. Stem Cells Transl. Med. 5: 1425–1439. [PubMed: 27388239]

28. Cheng L, Sharples RA, Scicluna BJ, and Hill AF. 2014 Exosomes provide a protective and enriched source of miRNA for biomarker profiling compared to intracellular and cell-free blood. J. Extracell. Vesicles 3.

29. Chen TS, Lai RC, Lee MM, Choo AB, Lee CN, and Lim SK. 2010 Mesenchymal stem cell secretes microparticles enriched in pre-microRNAs. Nucleic Acids Res. 38: 215–224. [PubMed: 19850715]

30. Alexander M, Hu R, Runtsch MC, Kagele DA, Mosbruger TL, Tolmachova T, Seabra MC, Round JL, Ward DM, and O'Connell RM. 2015 Exosome-delivered microRNAs modulate the inflammatory response to endotoxin. Nat. Commun. 6: 7321. [PubMed: 26084661]

31. Clark EA, Kalomoiris S, Nolta JA, and Fierro FA. 2014 Concise review: MicroRNA function in multipotent mesenchymal stromal cells. Stem Cells 32: 1074–1082. [PubMed: 24860868]

32. Adegani FJ, Langroudi L, Arefian E, Shafiee A, Dinarvand P, and Soleimani M. 2013 A comparison of pluripotency and differentiation status of four mesenchymal adult stem cells. Mol. Biol. Rep. 40: 3693–3703. [PubMed: 23275202]

33. Zhan M, Zhao X, Wang H, Chen W, Xu S, Wang W, Shen H, Huang S, and Wang J. 2016 miR-145 sensitizes gallbladder cancer to cisplatin by regulating multidrug resistance associated protein 1. Tumour Biol. 37: 10553–10562. [PubMed: 26852750]

34. Gao M, Miao L, Liu M, Li C, Yu C, Yan H, Yin Y, Wang Y, Qi X, and Ren J. 2016 miR-145 sensitizes breast cancer to doxorubicin by targeting multidrug resistance-associated protein-1. Oncotarget 7: 59714–59726. [PubMed: 27487127]
35. Lee RH, Yu JM, Foskett AM, Peltier G, Reneau JC, Bazhanov N, Oh JY, and Prockop DJ. 2014 TSG-6 as a biomarker to predict efficacy of human mesenchymal stem/progenitor cells (hMSCs) in modulating sterile inflammation in vivo. Proc. Natl. Acad. Sci. U S A 111: 16766–16771. [PubMed: 25385603]
36. Dominici M, Le Blanc K, Mueller I, Slaper-Cortenbach I, Marini F, Krause D, Deans R, Keating A, Prockop DJ, and Horwitz E. 2006 Minimal criteria for defining multipotent mesenchymal stromal cells. The International Society for Cellular Therapy position statement. Cytotherapy 8: 315–317. [PubMed: 16923606]
37. Bruno S, Grange C, Collino F, Deregibus MC, Cantaluppi V, Biancone L, Tetta C, and Camussi G. 2012 Microvesicles derived from mesenchymal stem cells enhance survival in a lethal model of acute kidney injury. PLoS One 7: e33115. [PubMed: 22431999]
38. Kips JC, Joos GF, De Lepeleire I, Margolskee DJ, Buntinx A, Pauwels RA, and Van der Straeten ME. 1991 MK-571, a potent antagonist of leukotriene D4-induced bronchoconstriction in the human. Am. Rev. Respir. Dis. 144: 617–621. [PubMed: 1892302]
39. Koley D, and Bard AJ. 2012 Inhibition of the MRP1-mediated transport of the menadione-glutathione conjugate (thiodione) in HeLa cells as studied by SECM. Proc. Natl. Acad. Sci. U S A 109: 11522–11527. [PubMed: 22679290]
40. Bruno S, Grange C, Deregibus MC, Calogero RA, Saviozzi S, Collino F, Morando L, Busca A, Falda M, Bussolati B, Tetta C, and Camussi G. 2009 Mesenchymal stem cell-derived microvesicles protect against acute tubular injury. J. Am. Soc. Nephrol. 20: 1053–1067. [PubMed: 19389847]
41. Gupta N, Su X, Popov B, Lee JW, Serikov V, and Matthay MA. 2007 Intrapulmonary delivery of bone marrow-derived mesenchymal stem cells improves survival and attenuates endotoxin-induced acute lung injury in mice. J. Immunol. 179: 1855–1863. [PubMed: 17641052]
42. Krasnodembskaya A, Song Y, Fang X, Gupta N, Serikov V, Lee JW, and Matthay MA. 2010 Antibacterial effect of human mesenchymal stem cells is mediated in part from secretion of the antimicrobial peptide LL-37. Stem Cells 28: 2229–2238. [PubMed: 20945332]
43. Wan M, Sabirsh A, Wetterholm A, Agerberth B, and Haeggstrom JZ. 2007 Leukotriene B4 triggers release of the cathelicidin LL-37 from human neutrophils: novel lipid-peptide interactions in innate immune responses. FASEB J. 21: 2897–2905. [PubMed: 17446260]
44. Wan M, Soehnlein O, Tang X, van der Does AM, Smedler E, Uhlen P, Lindbom L, Agerberth B, and Haeggstrom JZ. 2014 Cathelicidin LL-37 induces time-resolved release of LTB4 and TXA2 by human macrophages and triggers eicosanoid generation in vivo. FASEB J. 28: 3456–3467. [PubMed: 24736410]
45. Gennai S, Monsel A, Hao Q, Park J, Matthay MA, and Lee JW. 2015 Microvesicles Derived From Human Mesenchymal Stem Cells Restore Alveolar Fluid Clearance in Human Lungs Rejected for Transplantation. Am. J. Transplant. 15: 2404–2412. [PubMed: 25847030]
46. Cassatella MA, Mosna F, Micheletti A, Lisi V, Tamassia N, Cont C, Calzetti F, Pelletier M, Pizzolo G, and Krampera M. 2011 Toll-like receptor-3-activated human mesenchymal stromal cells significantly prolong the survival and function of neutrophils. Stem Cells 29: 1001–1011. [PubMed: 21563279]
47. Raffaghello L, Bianchi G, Bertolotto M, Montecucco F, Busca A, Dallegri F, Ottonello L, and Pistoia V. 2008 Human mesenchymal stem cells inhibit neutrophil apoptosis: a model for neutrophil preservation in the bone marrow niche. Stem Cells 26: 151–162. [PubMed: 17932421]
48. McGee JE, and Fitzpatrick FA. 1986 Erythrocyte-neutrophil interactions: formation of leukotriene B4 by transcellular biosynthesis. Proc. Natl. Acad. Sci. U S A 83: 1349–1353. [PubMed: 3006048]
49. Feinmark SJ, and Cannon PJ. 1986 Endothelial cell leukotriene C4 synthesis results from intercellular transfer of leukotriene A4 synthesized by polymorphonuclear leukocytes. J. Biol. Chem. 261: 16466–16472. [PubMed: 3023351]
50. Bigby TD, and Meslier N. 1989 Transcellular lipoxygenase metabolism between monocytes and platelets. J. Immunol. 143: 1948–1954. [PubMed: 2550547]

51. Zarini S, Gijon MA, Ransome AE, Murphy RC, and Sala A. 2009 Transcellular biosynthesis of cysteinyl leukotrienes in vivo during mouse peritoneal inflammation. Proc. Natl. Acad. Sci. U S A 106: 8296–8301. [PubMed: 19416808]
52. Capra V, Rovati GE, Mangano P, Buccellati C, Murphy RC, and Sala A. 2015 Transcellular biosynthesis of eicosanoid lipid mediators. Biochim. Biophys. Acta. 1851: 377–382. [PubMed: 25218301]
53. Marcus AJ, Broekman MJ, Safier LB, Ullman HL, Islam N, Sherhan CN, Rutherford LE, Korchak HM, and Weissmann G. 1982 Formation of leukotrienes and other hydroxy acids during platelet-neutrophil interactions in vitro. Biochem. Biophys. Res. Commun. 109: 130–137. [PubMed: 6297472]
54. Maugeri N, Evangelista V, Celardo A, Dell'Elba G, Martelli N, Piccardoni P, de Gaetano G, and Cerletti C. 1994 Polymorphonuclear leukocyte-platelet interaction: role of P-selectin in thromboxane B2 and leukotriene C4 cooperative synthesis. Thromb. Haemost. 72: 450–456. [PubMed: 7531878]
55. Mao YX, Xu JF, Seeley EJ, Tang XD, Xu LL, Zhu YG, Song YL, and Qu JM. 2015 Adipose Tissue-Derived Mesenchymal Stem Cells Attenuate Pulmonary Infection Caused by Pseudomonas aeruginosa via Inhibiting Overproduction of Prostaglandin E2. Stem Cells 33: 2331–2342. [PubMed: 25788456]
56. Aronoff DM, Canetti C, and Peters-Golden M. 2004 Prostaglandin E2 inhibits alveolar macrophage phagocytosis through an E-prostanoid 2 receptor-mediated increase in intracellular cyclic AMP. J. Immunol. 173: 559–565. [PubMed: 15210817]
57. Ham EA, Soderman DD, Zanetti ME, Dougherty HW, McCauley E, and Kuehl FA Jr. 1983 Inhibition by prostaglandins of leukotriene B4 release from activated neutrophils. Proc. Natl. Acad. Sci. U S A 80: 4349–4353. [PubMed: 6308617]
58. Nemeth K, Leelahavanichkul A, Yuen PS, Mayer B, Parmelee A, Doi K, Robey PG, Leelahavanichkul K, Koller BH, Brown JM, Hu X, Jelinek I, Star RA, and Mezey E. 2009 Bone marrow stromal cells attenuate sepsis via prostaglandin E(2)-dependent reprogramming of host macrophages to increase their interleukin-10 production. Nat. Med. 15: 42–49. [PubMed: 19098906]
59. Lee SP, Serezani CH, Medeiros AI, Ballinger MN, and Peters-Golden M. 2009 Crosstalk between prostaglandin E2 and leukotriene B4 regulates phagocytosis in alveolar macrophages via combinatorial effects on cyclic AMP. J. Immunol. 182: 530–537. [PubMed: 19109185]
60. Eckmann L, Stenson WF, Savidge TC, Lowe DC, Barrett KE, Fierer J, Smith JR, and Kagnoff MF. 1997 Role of intestinal epithelial cells in the host secretory response to infection by invasive bacteria. Bacterial entry induces epithelial prostaglandin h synthase-2 expression and prostaglandin E2 and F2alpha production. J. Clin. Invest. 100: 296–309. [PubMed: 9218506]
61. Araujo-Santos T, Prates DB, Franca-Costa J, Luz NF, Andrade BB, Miranda JC, Brodskyn CI, Barral A, Bozza PT, and Borges VM. 2014 Prostaglandin E2/leukotriene B4 balance induced by Lutzomyia longipalpis saliva favors Leishmania infantum infection. Parasit. Vectors 7: 601. [PubMed: 25526785]
62. Ziemann C, Schafer D, Rudell G, Kahl GF, and Hirsch-Ernst KI. 2002 The cyclooxygenase system participates in functional mdr1b overexpression in primary rat hepatocyte cultures. Hepatology 35: 579–588. [PubMed: 11870370]
63. Torky A, Raemisch A, Glahn F, and Foth H. 2008 Arachidonic acid pathway activates multidrug resistance related protein in cultured human lung cells. Arch. Toxicol. 82: 323–332. [PubMed: 17943274]
64. Surowiak P, Pawelczyk K, Maciejczyk A, Pudelko M, Kolodziej J, Zabel M, Murawa D, Drag M, Gansukh T, Dietel M, and Lage H. 2008 Positive correlation between cyclooxygenase 2 and the expression of ABC transporters in non-small cell lung cancer. Anticancer Res. 28: 2967–2974. [PubMed: 19031941]
65. Liu B, Qu L, and Tao H. 2009 Cyclo-oxygenase 2 up-regulates the effect of multidrug resistance. Cell Biol. Int. 34: 21–25. [PubMed: 20001974]
66. Shinohara H, Kuranaga Y, Kumazaki M, Sugito N, Yoshikawa Y, Takai T, Taniguchi K, Ito Y, and Akao Y. 2017 Regulated Polarization of Tumor-Associated Macrophages by miR-145 via

Colorectal Cancer-Derived Extracellular Vesicles. J. Immunol. 199: 1505–1515. [PubMed: 28696255]

67. Fang X, Abbott J, Cheng L, Colby JK, Lee JW, Levy BD, and Matthay MA. 2015 Human Mesenchymal Stem (Stromal) Cells Promote the Resolution of Acute Lung Injury in Part through Lipoxin A4. J. Immunol. 195: 875–881. [PubMed: 26116507]
68. Tsoyi K, Hall SR, Dalli J, Colas RA, Ghanta S, Ith B, Coronata A, Fredenburgh LE, Baron RM, Choi AM, Serhan CN, Liu X, and Perrella MA. 2016 Carbon Monoxide Improves Efficacy of Mesenchymal Stromal Cells During Sepsis by Production of Specialized Proresolving Lipid Mediators. Crit. Care Med. 44: e1236–e1245. [PubMed: 27513357]
69. Russell CD, and Schwarze J. 2014 The role of pro-resolution lipid mediators in infectious disease. Immunology 141: 166–173. [PubMed: 24400794]

Key Points:

1. MSC EV may stimulate increased antimicrobial activity during bacterial pneumonia.
2. Increased antimicrobial activity is associated with increased LTB_4 production.
3. MSC EV may increase LTB_4 production via transfer of miR145 to target cells.

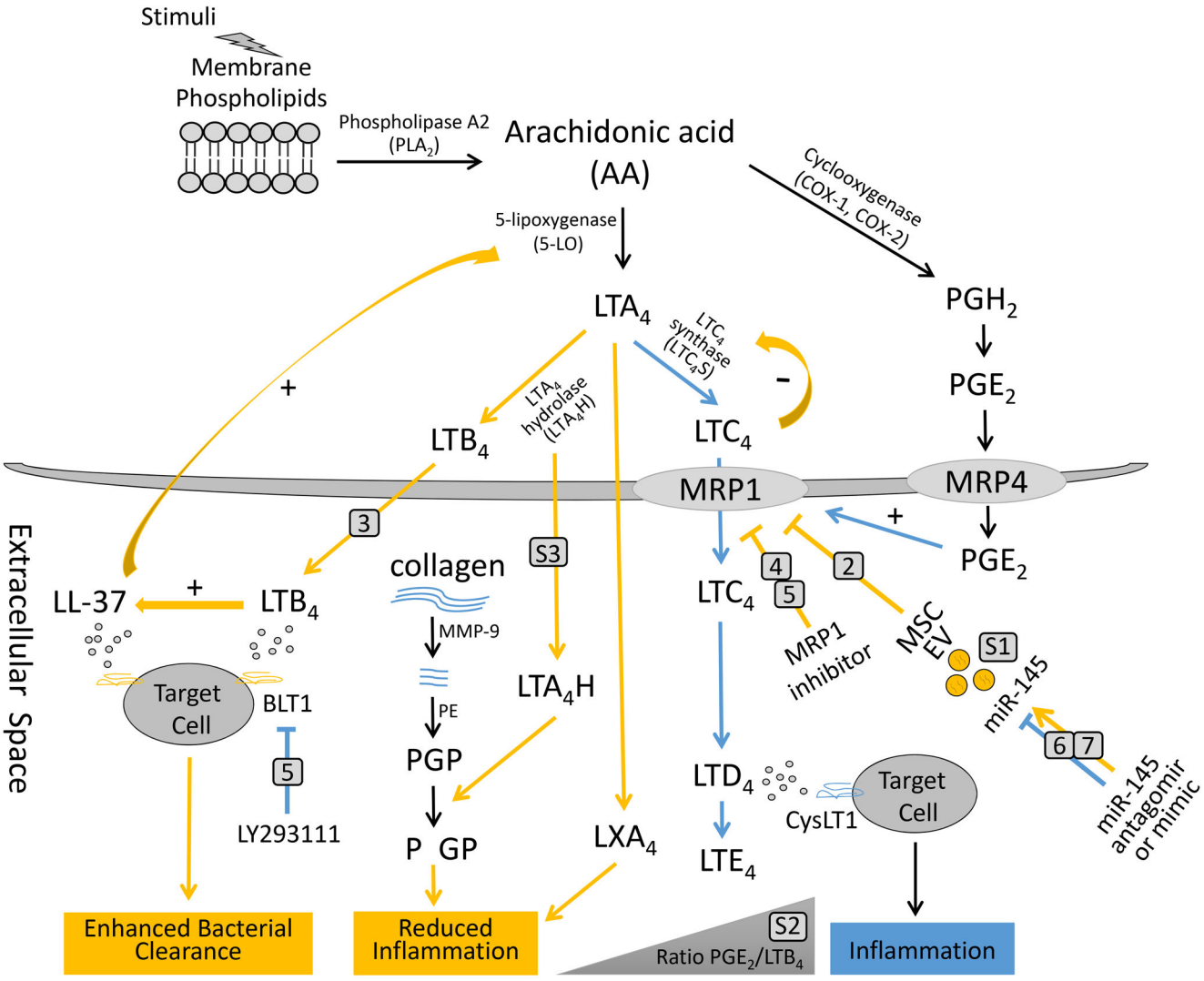

FIGURE 1. Role of Leukotrienes in the Antimicrobial Activity of MSC or MSC EV.

A schematic illustration of the possible mechanisms by which MSC or MSC EV increase bacteria killing. Numbers 2-7 refer to subsequent figures as a mechanism of MRP1 inhibition by MSC or MSC EV.

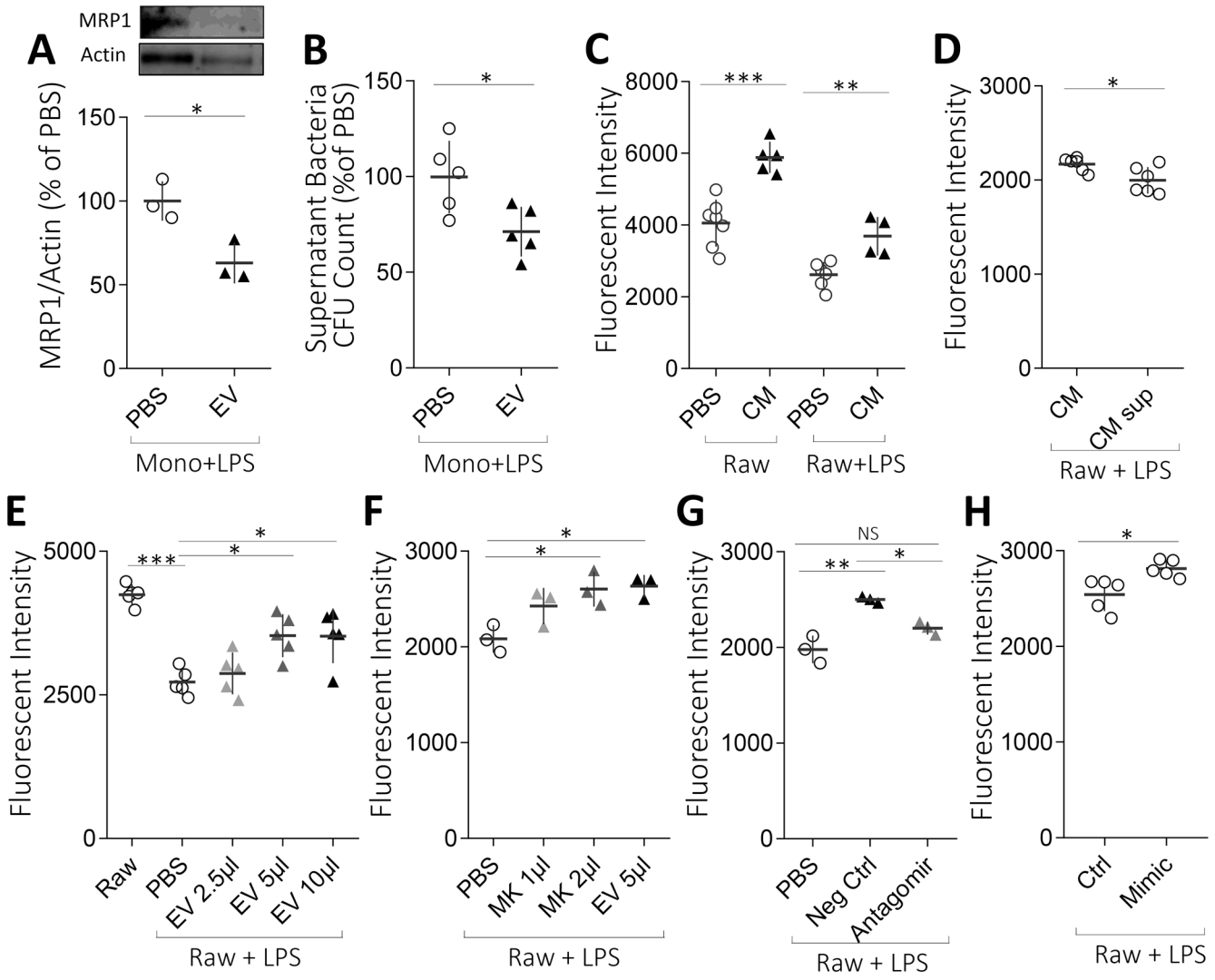

FIGURE 2. MSC EV Decreased *E.coli* Bacterial CFU Levels and MRP1 Protein Levels & MRP1 Activity.

(**A**) Administration of MSC EV decreased MRP1 protein level (Western blot) compared to controls, human monocytes exposed to LPS alone. *n* = 3. (**B**) Administration of MSC EV increased human monocyte phagocytosis of *E.coli* bacteria *in vitro* compared to PBS. The decrease in bacterial CFU counts was associated with decrease in MRP1 protein levels. *n* = 5. (**C**) A fluoroimetric MDR assay kit was used to determine MRP1 pump function; in the assay, cellular fluorescence increases if MRP1 activity is decreased. MSC CM decreased MRP1pump activity in Raw267.4 cells with or without LPS stimulation, suggesting that either a soluble factor or EV may be involved. *n* = 4-7. (**D**) MSC CM had a stronger effect on decreasing MRP1 pump activity in Raw267.4 cells compared to MSC CM supernatant (with EV removed). *n* = 6. (**E**) MSC EV decreased MRP1 pump activity in Raw267.4 cells stimulated with LPS in a dose dependent manner. *n* = 5. (**F**) MK-571 decreased MRP1 pump activity in Raw267.4 cells stimulated with LPS in a dose dependent manner. *n* = 3. (**G**) EV transfected with miR negative control decreased MRP1 pump activity. This effect was abolished when miR-145 antagomir was transfected into EV. *n* = 3. (**H**) Raw264.7 cells

transfected with miR-145 mimic decreased MRP1 pump activity compared to that of negative control. n = 3-7. Data were expressed as mean ± SD. Student's t-test was performed on Figures (A -D, H). 1-way ANOVA with Bonferroni's correction was performed on Figures (E-G). *, $p < 0.05$, **, $p < 0.01$, and ***, $p < 0.001$. Raw, Raw267.4 cells; MK, MK-571; Neg Ctrl, MSC EV transfected with miR antagomir negative control; Antagomir, MSC EV transfected with miR-145 antagomir; Ctrl, Raw cells transfected with miR mimic negative control; Mimic, Raw cells transfected with miR-145 mimic.

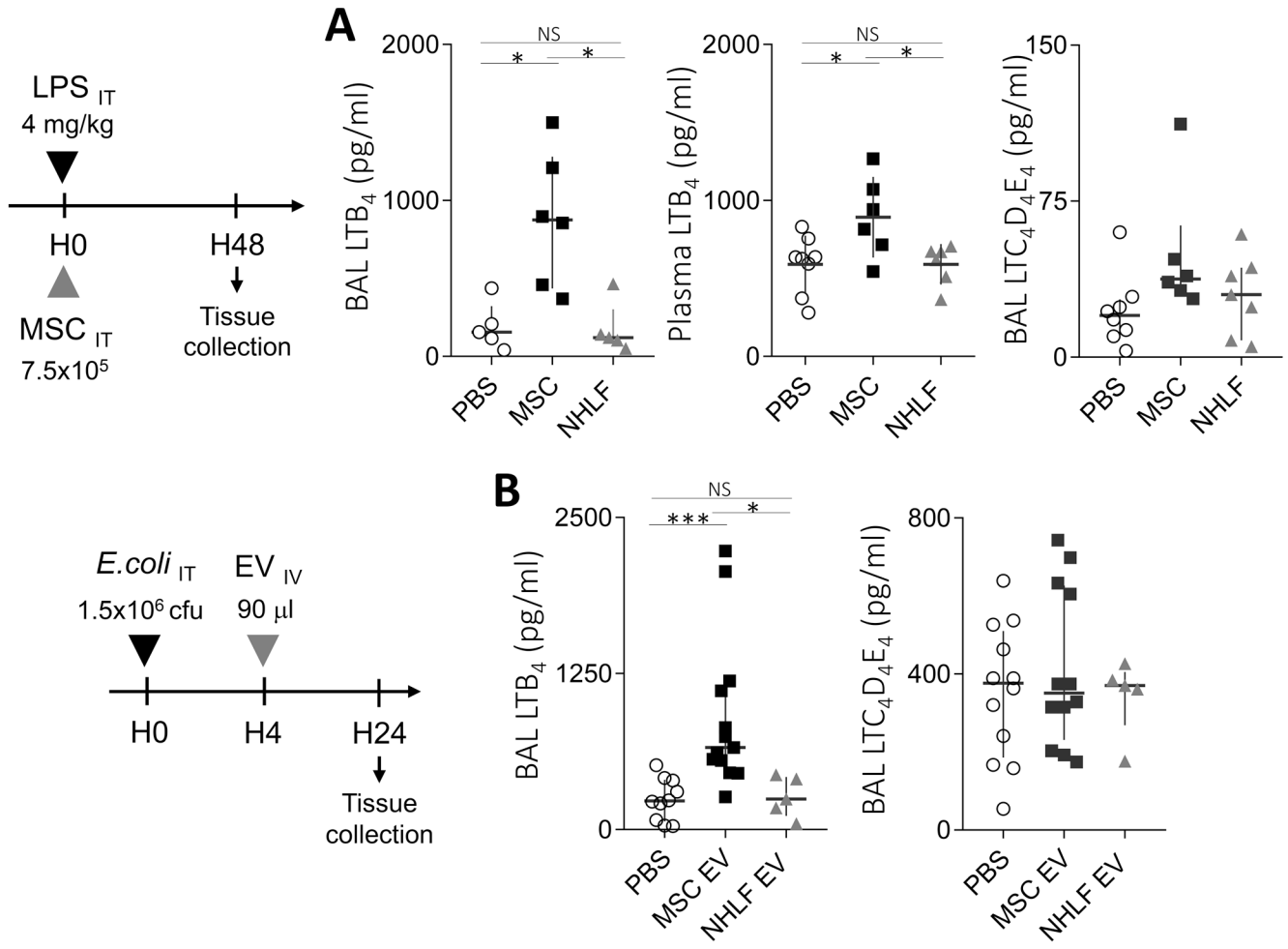

FIGURE 3. MSC or MSC EV Administration Increased LTB_4 levels in the BALF of Mice Injured with LPS or *E.coli* Bacterial Induced Lung Injury.

(**A**) Treatment with MSC significantly increased LTB_4 levels in BALF of mice injured with intra-tracheal LPS at 48 h (Kruskal-Wallis test with Dunn's correction). Plasma levels of LTB_4 were significantly increased with administration of MSC as well (1-way ANOVA with Bonferroni's correction). There were no significant differences in CysLTs level in all groups (Kruskal-Wallis test with Dunn's correction). n = 5-8. (**B**) Administration of MSC EV as therapy significantly increased LTB_4 levels in BALF of mice injured with intra-tracheal *E.coli* pneumonia at 24 h. Administration of NHLF or its released EV had no significant effect on LTB_4 levels. Data were mean ± SD or median with IQR. There were no significant differences in CysLTs level in all groups. n = 5-13. Kruskal-Wallis test with Dunn's correction. *, $p < 0.05$ and ***, $p < 0.001$.

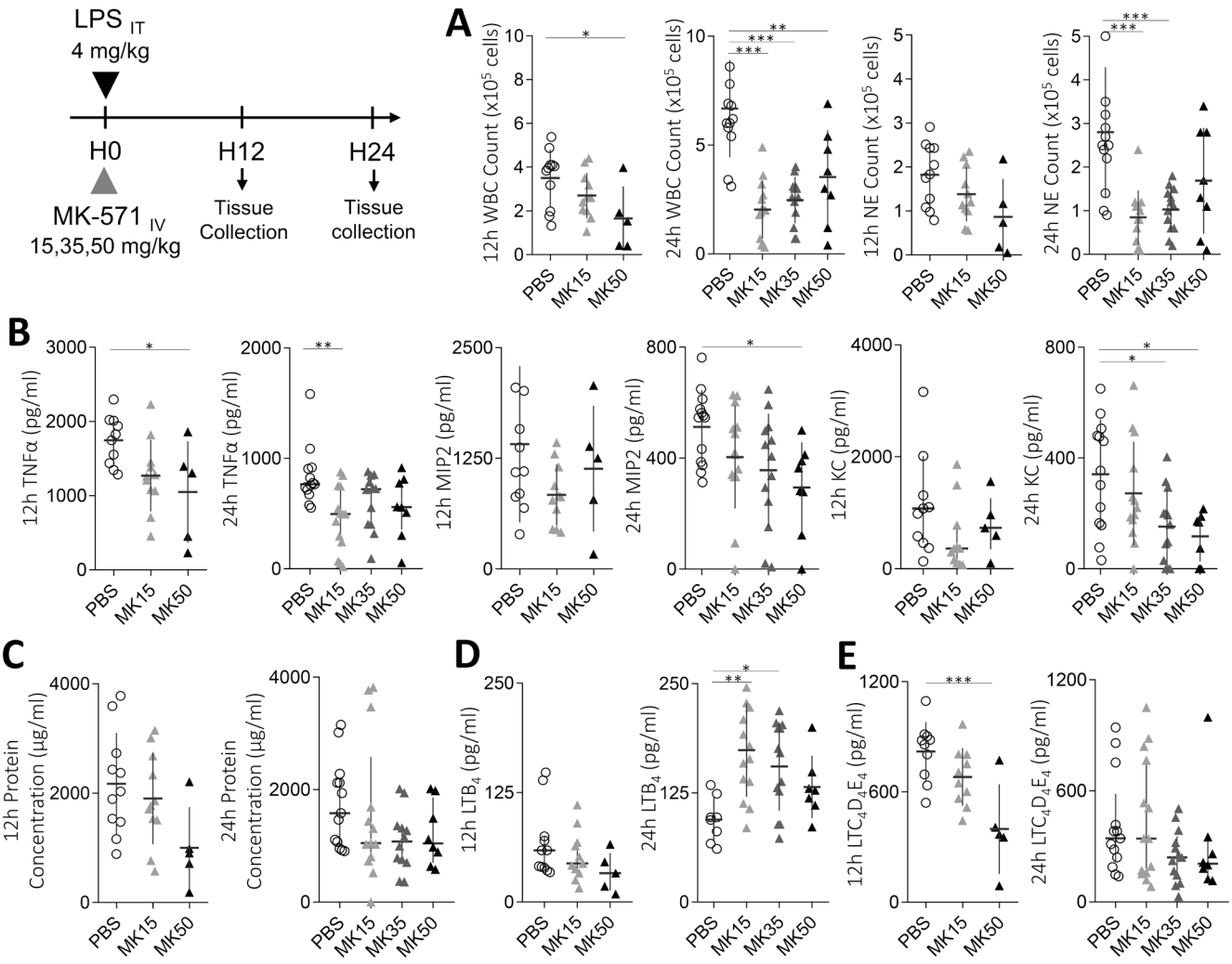

FIGURE 4. Administration of MK-571 Decreased LPS Induced Acute Lung Injury.

MK-571 administration significantly (**A**) reduced the influx of inflammatory cells, (**B**) down-regulated pro-inflammatory cytokines (TNFα, MIP-2, and KC), and was associated with a trend in reducing (**C**) total protein levels in the injured alveolus in a dose dependent manner. Compared to LPS-injured mice, MK-571 treatment increased LTB_4 levels at 24 h (**D**), which was associated with reduced cysteinyl LTs levels (**E**). Data were expressed as mean ± SD or median with IQR, n = 5-11 (12 h time point) and 7-14 (24 h time point). 1-way ANOVA with the Bonferroni's correction analyses was performed for WBC, NE, MIP-2, 12 h TNFα, 24 h KC, 12 h protein concentration, 24 h LTB_4, 12 h CysLTs; Kruskal-Wallis test with Dunn's correction analyses was performed for 24 h TNFα, 12 h KC, 24 h protein concentration, 12 h LTB_4, 24 h CysLTs. *, $p < 0.05$, **, $p < 0.01$, and ***, $p < 0.001$.

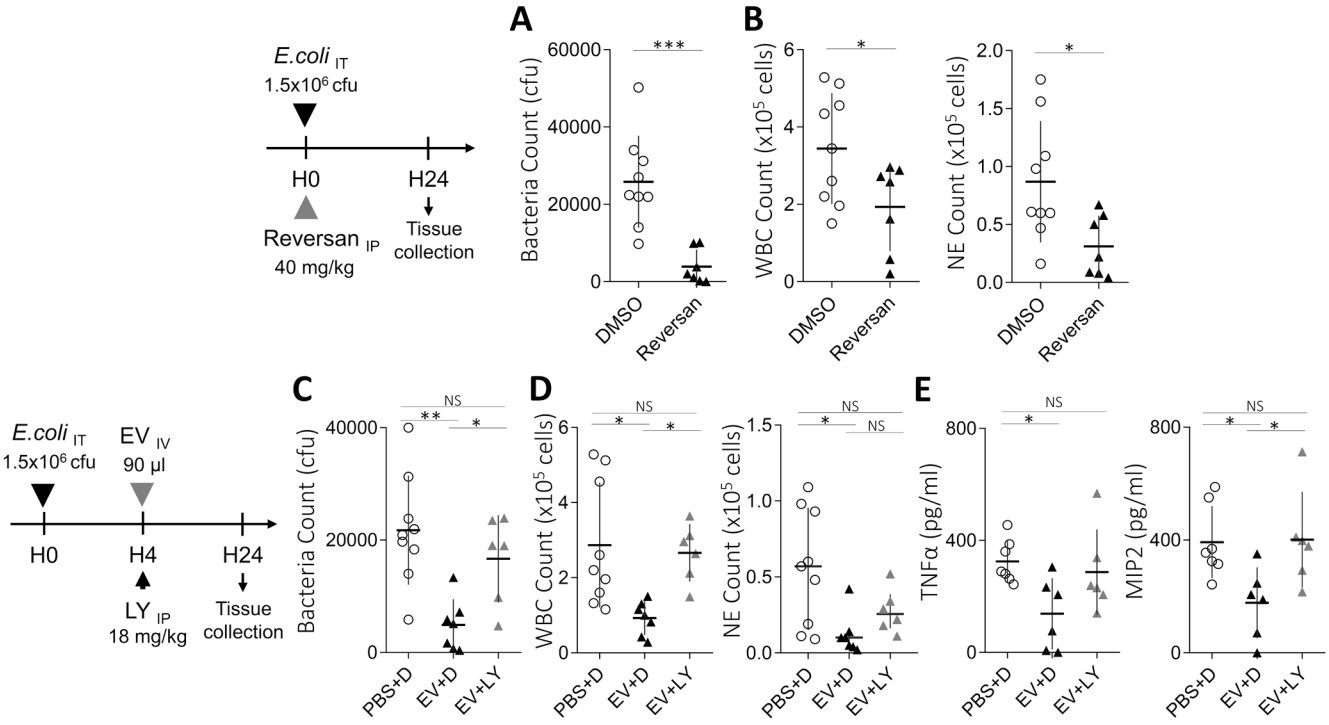

FIGURE 5. Role of MRP1 Inhibition and LTB_4 in the Antimicrobial Activity of MSC EV.

Administration of Reversan, a specific inhibitor of MRP1, in mice with *E.coli* pneumonia decreased (**A**) total bacterial CFU counts and (**B**) the influx of inflammatory cells, corroborating the effects seen with MK-571. Administration of LY293111, a LTB_4 Receptor 1 antagonist, reduced the therapeutic effects of MSC EV in mice injured with *E.coli* pneumonia in terms of reducing (**C**) total bacterial CFU counts, (**D**) the influx of inflammatory cells, and (**E**) inflammatory cytokines/chemokines in the BALF. Data were expressed as mean ± SD or median with IQR, n = 6-9. Student's t-test was performed for Figures (A-B); 1-way ANOVA with the Bonferroni's correction was performed for Figures (C, D: WBC count, and E); Kruskal-Wallis test with Dunn's correction (D: NE count). *, $p < 0.05$, **, $p < 0.01$, and ***, $p < 0.001$. LY, LY293111. D, DMSO.

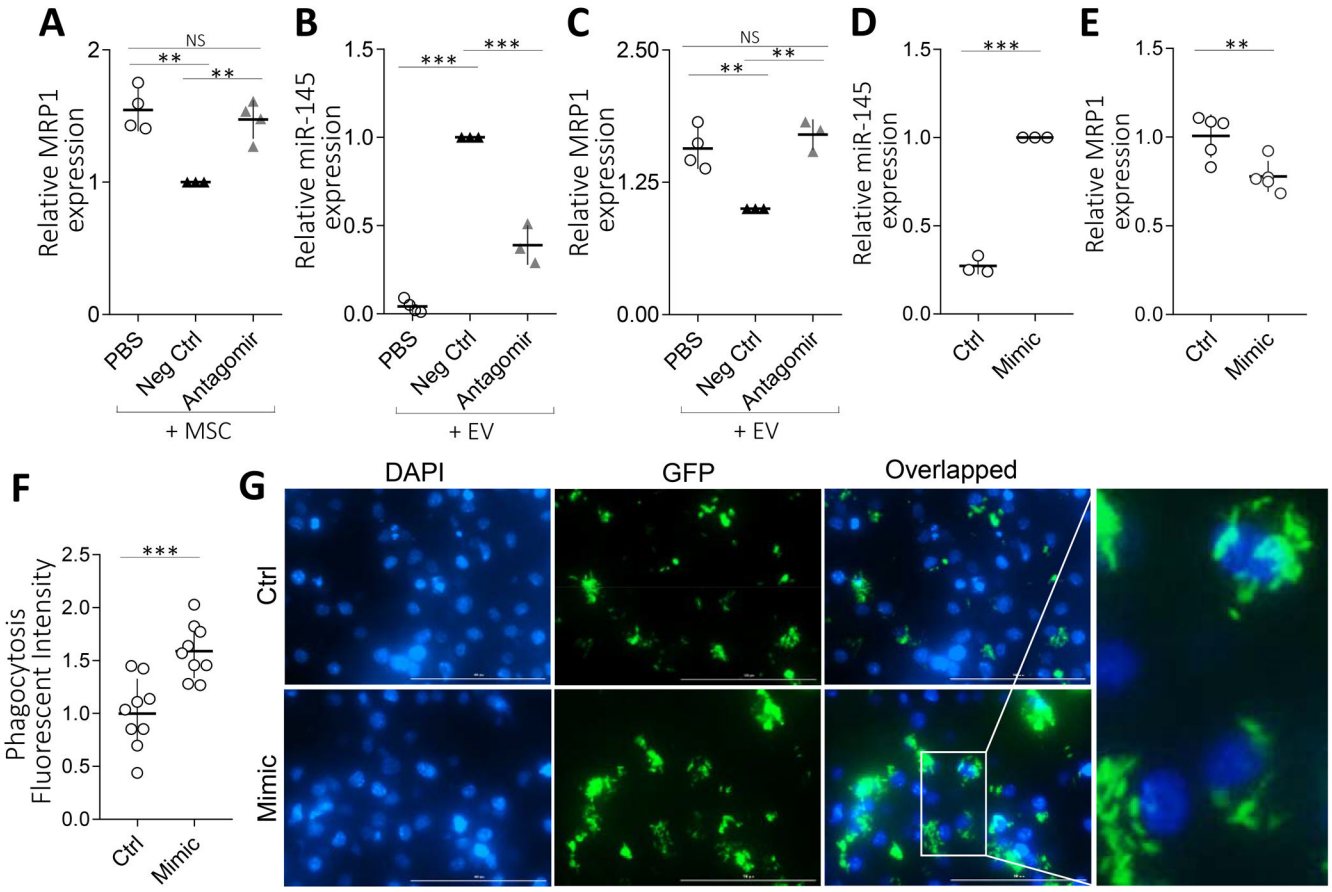

FIGURE 6. MiR-145 Regulates the Expression of MRP1 and the Phagocytic Activity of Raw267.4 Cells.

(**A**) Administration of MSC suppressed MRP1 expression in part by transfer of miR-145. Similar to MSC, administration of MSC EV significantly increased (**B**) miR-145 levels, which was associated with a decrease in (**C**) MRP1expression. MSC EV transfected with miR-145 antagomir eliminated the effect of MSC EV on MRP1 expression (**D**). Raw264.7 cells transfected with miR-145 mimic increased miR-145 levels, which was associated with a decrease in (**E**) MRP1 expression. (**F**) Raw267.4 cells transfected with miR-145 mimic had increased phagocytosis activity against GFP-labelled *E.coli* bacteria. (**G**) Representative images of phagocytosis of GFP labelled *E. coli* bacteria by Raw267.4 cells, pre-transfected by miR-145 mimic or negative control. Bar = 100 μm. n = 3-5 for A-E. n = 9 for F. Data were expressed as mean ± SD. 1-way ANOVA with the Bonferroni's correction was performed for Figures (A-C), and Student's t-test was performed for Figures (D-F). **, $p < 0.01$, and ***, $p < 0.001$.

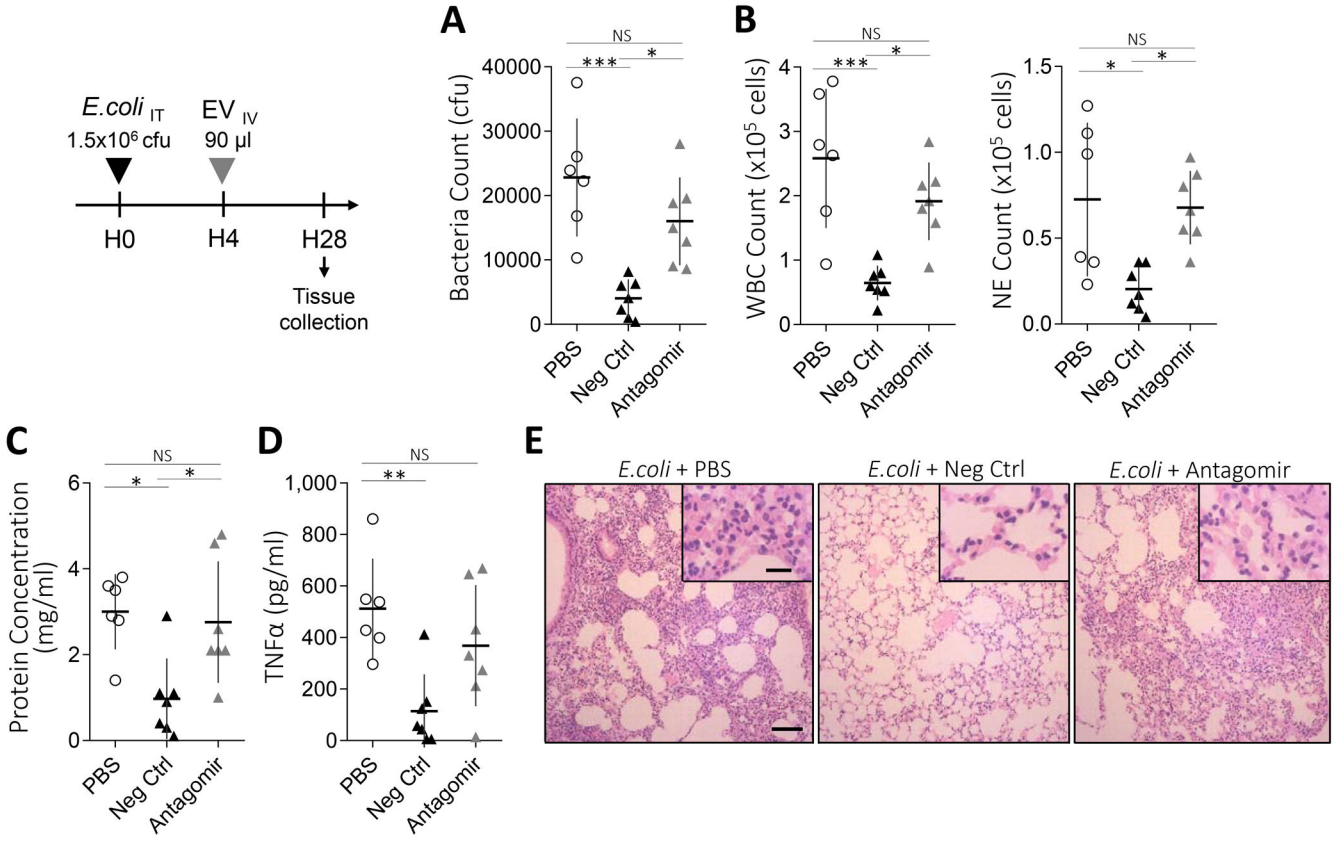

FIGURE 7. Knockdown of miR-145 in MSC EV Inhibited the Antimicrobial effect of MSC EV on *E.coli* Bacterial Growth.

Compared to negative control transfected MSC EV (Neg Ctrl), miR-145 antagomir transfected MSC EV (Antagomir) reduced the therapeutic effects of MSC EV in terms of reducing (**A**) total bacterial CFU counts, (**B**) the influx of total WBC and neutrophils, (**C**) total protein concentration, and **D**) TNFα in the BALF. (**E**) Representative H&E staining of lung sections. Bars 50 μm and 10 μm (insert). Data were expressed as mean ± SD, $n = 6$-7. 1-way ANOVA with the Bonferroni's correction. *, $p < 0.05$, **, $p < 0.01$, and ***, $p < 0.001$.